PACS №: 41.20.Gz
G.R. Turner
South African Nuclear Energy Corporation,
P. O. Box 582, Pretoria, 0001
South Africa

# Inductance Calculations For Helical Magnetocumulative Generators

## Contents



## Abstract

Modifications to the well known technique for calculating the inductance of a circularly symmetric conducting structure, such as that of a magnetocumulative generator, are presented. The presented method is verified both theoretically and experimentally.

## 1. Introduction

Novac *et al* [1] have presented a method for the analysis of a variable-pitch multi-section helical magnetocumulative generator (MCG). This method requires that the helical stator and cylindrical armature be broken down into a number of parallel coaxial conducting filaments, and that the self inductance of each circular filament and the mutual inductance it shares with all other filaments be calculated. The method for the calculation of the mutual inductance between two filaments is well known. Grover [2], Smythe [3] and Knoepfel [4] (to name a few) present equivalent methods requiring the solution of elliptic integrals. Indeed, Grover comments that "Since the original formula given by Maxwell, numerous series developments have appeared ... so that no less than a hundred formulas have been published". The method of Novac is no different, with the exception that Novac's equation 9 appears to have incurred a typing error. This error has propagated through to the work of Altgilbers *et al* [5].

In this paper yet another method is presented. For those new to MCG simulations the method is derived from first principles. For those relying on fast computer simulation techniques the method uses two alternative elliptic integrals — the complete Legendre elliptic integral of the first kind $F(\psi, k)$, and a linear combination of the Legendre elliptic integrals of the first and second kind $D(\psi, k)$. Although little different, the choice of these integrals (in preference to the accepted first and second Legendre elliptic integrals) facilitates a subtle improvement in the prescribed method for numeric solution of elliptic integrals. Namely $F(\psi, k)$ and $D(\psi, k)$ may be solved simultaneously.

## 2. Method

Figure 1 shows two parallel coaxial conducting filaments, one of radius $r_i$ the other of radius $r_j$, separated by distance $d_{ij}$. For the purpose of this problem the lower filament carries current $I$ and the upper filament defines the boundary of an enclosed surface $\mathbf{S}$.

Fig. 2 shows the two circular filaments observed from above the $xy$-plane. The angle $\theta$ is subtended between the vectors PO and QO projected onto the $xy$-plane.

By definition magnetic flux density $\mathbf{B} = \nabla \times \mathbf{A}$, where $\mathbf{A}$ is the magnetic vector potential. Since $\Phi = \int\limits_S \mathbf{B} \cdot \mathbf{dS}$ it is easily shown (by means of Stokes'

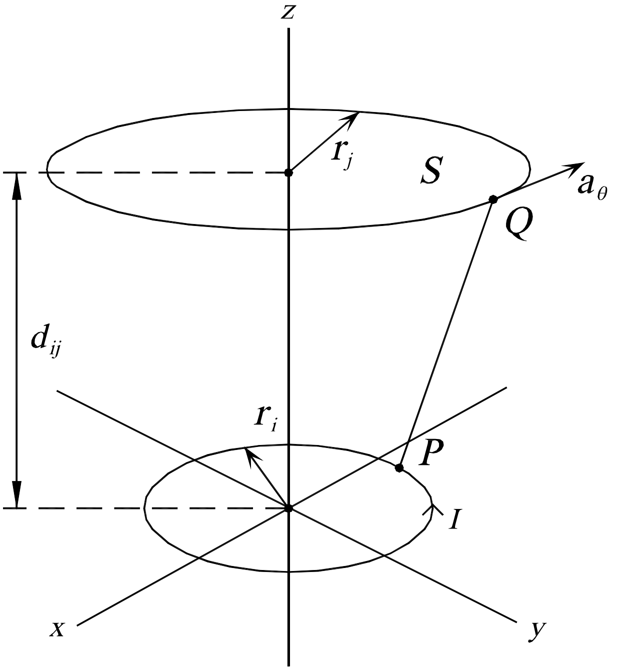


Fig. 1. Two conducting filaments, radius $r_i$ and $r_j$, centred on the $z$-axis and separated by distance $d_{ij}$.

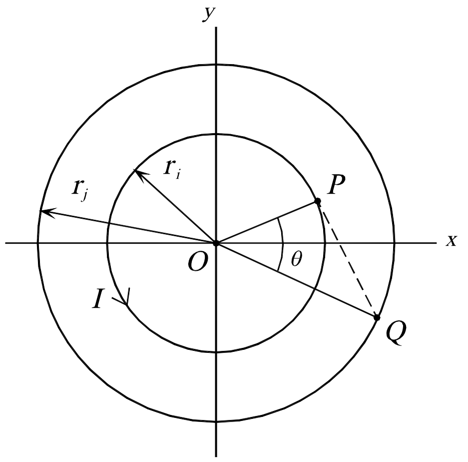


Fig. 2. The two conducting filaments, radius $r_i$ and $r_j$, viewed from above the $xy$-plane.

theorem) that:

$$\Phi = \oint \mathbf{A} \cdot \mathbf{dl} \qquad (1)$$

where $\Phi$ is the total magnetic flux (due to current $I$ flowing in the lower filament) coupled to the surface $\mathbf{S}$ (bounded by the upper filament), and:

$$\mathbf{dl} = r_j d\theta \mathbf{a}_\theta \qquad (2)$$

where $\mathbf{a}_\theta$ is the unit vector in the $\theta$ direction. Since the current through the lower filament is by definition a line current, then:

$$\mathbf{A} = \frac{\mu_0}{4\pi} \oint \frac{I\mathbf{dl}}{r} \qquad (3)$$

where in this case:

$$\mathbf{dl} = r_i d\theta \mathbf{a}_\theta \qquad (4)$$

$\mu_0$ is the magnetic permeability of free space and $r$ is the scalar distance between the current element $I\mathbf{dl}$ (point $P$ on the lower filament) and that point at which the magnetic vector potential $\mathbf{A}$ is determined (point $Q$ on the upper filament). Hence:

$$r = |P - Q| = \sqrt{d_{ij}^2 + r_i^2 + r_j^2 - 2r_i r_j \cos\theta}. \qquad (5)$$

The contribution to the magnetic vector potential $\mathbf{A}$ at the point $Q$ (in the $\mathbf{a}_\theta$ direction) as the point P is moved around the lower filament, is proportional to $\cos\theta$. Consequently, from (3) and (5):

$$\mathbf{A} = \frac{\mu_0 I r_i}{4\pi} \int\limits_{\theta=0}^{\theta=2\pi} \frac{\cos\theta d\theta \mathbf{a}_\theta}{\sqrt{d_{ij}^2 + r_i^2 + r_j^2 - 2r_i r_j \cos\theta}}. \qquad (6)$$

Letting $\theta = 2\alpha$ and substituting $\cos(2\alpha) = 1 - 2\sin^2\alpha$ into (6):

$$\mathbf{A} = \frac{\mu_0 I r_i}{4\pi} \times \int\limits_{\theta=0}^{\theta=2\pi} \frac{(1 - 2\sin^2\alpha) 2 d\alpha \mathbf{a}_\theta}{\sqrt{(d_{ij}^2 + (r_i - r_j)^2) + 4 r_i r_j \sin^2\alpha}}. \qquad (7)$$

Substituting $\sin^2\alpha + \cos^2 = 1$ into (7):

$$\mathbf{A} = \frac{\mu_0 I r_i}{2\pi\sqrt{d_{ij}^2 + (r_i - r_j)^2}} \times \int\limits_{\alpha=0}^{\alpha=\pi} \frac{(1 - 2\sin^2\alpha) d\alpha \mathbf{a}_\theta}{\sqrt{\cos^2\alpha + k_c^2 \sin^2\alpha}} \qquad (8)$$

where:

$$k_c^2 = \frac{d_{ij}^2 + (r_i + r_j)^2}{d_{ij}^2 + (r_i - r_j)^2}. \qquad (9)$$

The integrand of (8) is a symmetric function. Hence:

$$\mathbf{A} = \frac{\mu_0 I r_i}{\pi\sqrt{d_{ij}^2 + (r_i - r_j)^2}} \times \int\limits_{\alpha=0}^{\alpha=\pi/2} \frac{(1 - 2\sin^2\alpha) d\alpha \mathbf{a}_\theta}{\sqrt{\cos^2\alpha + k_c^2 \sin^2\alpha}}. \qquad (10)$$

The magnetic vector potential $\mathbf{A}$, calculated at the point $Q$, is independent of the absolute position of the points $P$ and $Q$ over the $xy$-plane, depending only on the *relative* angle $\theta$ subtended between the two points and the origin. Consequently the magnitude of magnetic vector potential $\mathbf{A}$ is constant around the circular path defined by the upper filament. Hence, from (1):

$$\Phi = \mathbf{A}\cdot \int\limits_{\psi=0}^{\psi=2\pi} r_j d\theta \mathbf{a}_\theta = 2\pi r_j (\mathbf{A}\cdot\mathbf{a}_\theta). \quad (11)$$

Since by definition $M_{ij} = \Phi_j / I_i$, where $M_{ij}$ is the mutual inductance between the $i^{\text{th}}$ and $j^{\text{th}}$ filament, then from (10) and (11):

$$M_{ij} = \frac{2\mu_0 r_i r_j}{\sqrt{d_{ij}^2 + (r_i - r_j)^2}} \left( \int\limits_{\alpha=0}^{\alpha=\pi/2} \frac{d\alpha}{\sqrt{\cos^2\alpha + k_c^2 \sin^2\alpha}} - 2 \int\limits_{\alpha=0}^{\alpha=\pi/2} \frac{\sin^2\alpha . d\alpha}{\sqrt{\cos^2\alpha + k_c^2 \sin^2\alpha}} \right). \quad (12)$$

The first integral term in (12) is the Legendre elliptic integral of the first kind, denoted $F(\phi, k)$, where $k^2 = 1 - k_c^2$. The integral is performed between 0 and $\pi/2$ and is consequently termed the *complete elliptic integral of the first kind*. The second integral term is a linear combination of the complete elliptic integrals of the *first and second kind*, denoted $D(\phi, k)$. These elliptic integrals cannot be solved analytically and must be solved numerically. Press *et al* [6], as cited by Novac, present an algorithm for the solution to the complete elliptic integral of any kind, denoted $cel(k_c, p, a, b)$. Consequently, from equation 12:

$$M_{ij} = \frac{2\mu_0 r_i r_j}{\sqrt{d_{ij}^2 + (r_i - r_j)^2}} \times \left( F\left(\frac{\pi}{2}, k\right) - 2D\left(\frac{\pi}{2}, k\right) \right) \quad (13)$$

where according to Press:

$$\begin{aligned} F\left(\frac{\pi}{2}, k\right) &= cel(k_c, 1, 1, 1), \\ D\left(\frac{\pi}{2}, k\right) &= cel(k_c, 1, 0, 1). \end{aligned} \quad (14)$$

Due to the similarity in coefficients a computer code derived from Press was constructed whereby $cel(k_c, 1, 1, 1)$ and $cel(k_c, 1, 0, 1)$ could be solved for simultaneously.

# 3. Results

Although the above formulation was intended for use with more complicated structures of non-linear pitch, it was decided that (13) would be verified by means of comparison to two simple $N$-turn inductors of circular cross-section, namely a simple solenoid and a *pancake* coil. These two inductors were chosen specifically due to the abundance of pocket-book type inductance calculations to which equation (13) can be compared. Each turn of the inductor was approximated as one filament. The EMF $V$ measured across an inductor comprised of $N$ series connected filaments is the sum of the EMF due to each filament, where the EMF across each filament is the sum of the EMF due to a particular filament's self and mutual inductance components. Hence:

$$V = \sum_{i=1}^{i=N} \sum_{j=1}^{j=N} \left( M_{ij} \frac{dI_j}{dt} \right). \quad (15)$$

However, since current $I$ flows through all filaments:

$$V = \left( \sum_{i=1}^{i=N} \sum_{j=1}^{j=N} M_{ij} \right) \frac{dI}{dt}. \quad (16)$$

The self inductance $L$ of the complete inductor is therefore:

$$L = \sum_{i=1}^{i=N} \sum_{j=1}^{j=N} M_{ij}. \quad (17)$$

Note: $M_{ij}$, where $i = j$, is simply the self inductance of the filament, where $M_{ij(i=j)}$ of the $i^{\text{th}}$ filament was calculated using Grover's equation:

$$M_{ij(i=j)} = \mu_0 r_i \ln\left(\frac{8r_i}{r_c} - 1.75\right) \quad (18)$$

where $r_c$, the radius of a filament, was set to $0.4l/N$, which, for a solenoid of length $l$, took into account space between windings for insulation. All units are SI.

The self inductance of an $N$-turn solenoid, length $l$, radius $r$, was calculated using Kaufman's equation [7]:

$$L = 3.94 \times 10^{-5} \frac{r^2 N^2}{(9r + 10l)} \quad (19)$$

where in this case $r = r_i = r_j$. Fig. 3 shows a plot of equations (17) and (19) as a function of the number of turns $N$ between $N = 150$ and $N = 250$, The solenoid radius and winding pitch were arbitrarily set to 20 mm and 0.7 mm respectively.

Since the inductance of a solenoid is approximately proportional to $N^2/l$, and in this particular case $N$ is proportional to $l$ (since the winding pitch is constant), $L$ is expected to increase linearly with increased number of turns. This is as indicated by figure 3 for both equations (17) and (19).

The second inductor examined was the spiral or *pancake* coil. The pancake coil is, as its name suggests, a flat spiral of wire, wound one turn over the next, starting at initial radius $r_a$ and ending at final radius $r_b$. The inductance of the pancake coil was again calculated using Kaufman's equation:

$$L = 3.94 \times 10^{-5} \frac{(r_b + r_a) N^2}{\left(16 + 44\left(\frac{r_b - r_a}{r_b + r_a}\right)\right)}. \quad (20)$$

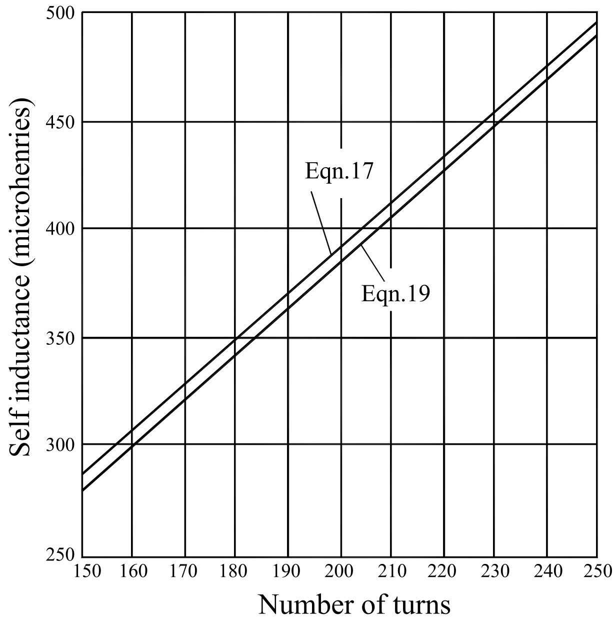


Fig. 3. Self inductance of a simple solenoid calculated using equations (17) and (19), as a function of number of turns.

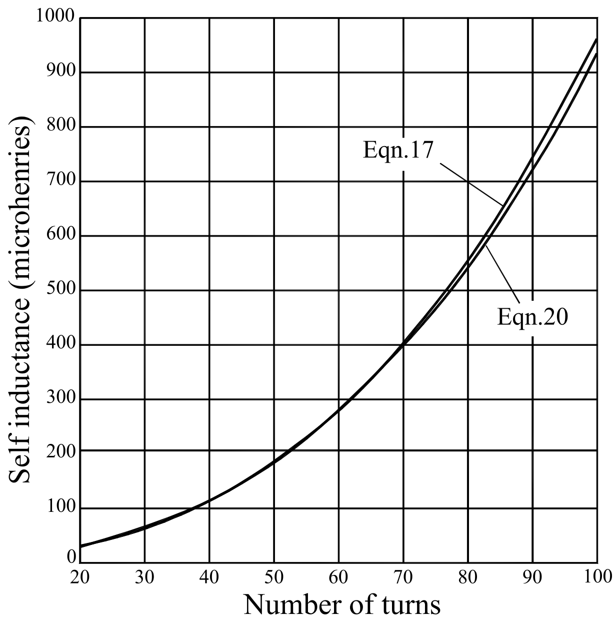


Fig. 4. Self inductance of a pancake coil calculated using equations (17) and (20), as a function of number of turns.

Since equation (13) is intended for use with filaments of varying radial (as well as lateral) spacing, the self-inductance of a spiral coil was modelled similarly to the simple solenoid, and compared to equation (20). Fig. 4 shows a plot of equations (17) and (20) as a function of the number of turns $N$ between $N = 20$ and $N = 100$. Each turn was again approximated by a single filament. The filament spacing was set to 1 mm,

Table 1. Measurement and calculation of the self inductance of a conical inductor as a function of the number of turns.

| Number of turns ($N$) | Measured Inductance ($\mu$H) | Calculate Inductance ($\mu$H) |
|---|---|---|
| 80 | 21 | 20.6 |
| 120 | 63 | 61.8 |
| 160 | 139 | 137.8 |
| 200 | 258 | 259.3 |
| 240 | 437 | 436.9 |
| 280 | 678 | 681.3 |
| 320 | 999 | 1000.3 |

and the initial radius $r_a$ was set to 20 mm.

To further facilitate the verification of the above method a comparison was made to data collected from a conical coil, manufactured from 0.4 mm diameter enamelled copper wire wound over a wooden mandrel. The conical mandrel, half-angle $15^0$, length 120 mm, was turned to size on a lathe. A perfect point could not be formed at the apex of the cone due to the limited strength of the wood from which the mandrel was turned. Consequently the radius of the first turn was restricted to 1.2 mm. The final radius of the cone, that is the radius of the $320^{\text{th}}$ turn, was $\sim$ 33.5 mm. The inductance of the conical coil was measured using a digital RCL meter at a frequency of 100 Hz, between 80 and 320 turns, at intervals of 40 turns. Table 1 shows the measured and calculated inductance values as a function of number of turns.

Figure 5 shows a plot of the calculated inductance as a function of number of turns for the conical inductor. The measured data points from Table 1 have been included. The maximum discrepancy between the predicted and measured values is 1.9 %. It is concluded, therefore, that the method presented for the calculation of the inductance of an arbitrary circularly symmetric conducting structure is reasonably accurate and reliable.

Note: The presented method requires an inductor or inductive structure (such as an MCG) to be broken down into a number of filaments. In the three cases considered, each winding was approximated as a single filament. This was considered acceptable since the current density through each turn of wire was assumed to be constant at a frequency as low as 100 Hz. However, at higher frequencies where the skin effect and the consequent non-uniform distribution of current through the windings is expected, each winding may be divided into a number of uniform

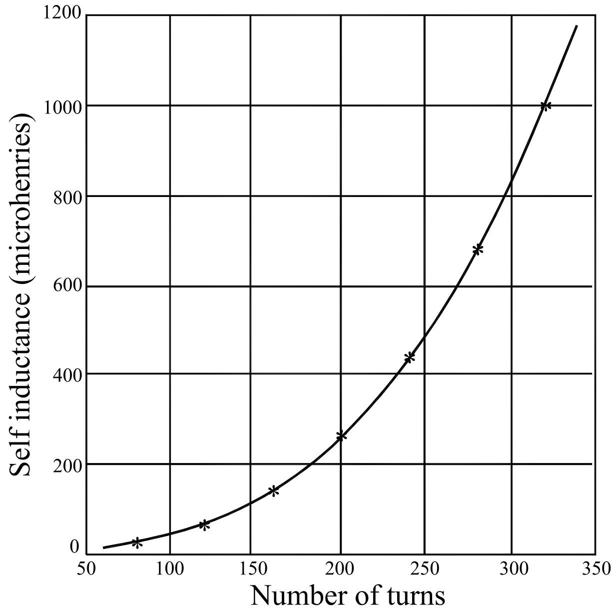


Fig. 5. Calculated self inductance of a conical inductor as a function of number of turns, measured values included.

current density filaments. Given the rapidly increasing speed and power of desktop computers, the number of filaments into which any given MCG stator turn or armature segment may be divided is large, while still maintaining a short code runtime. This technique has been implemented in MCG simulations where a correct understanding of high frequency effects is essential.

## 4. Conclusions

A method for the calculation of the inductance of a circularly symmetric coaxial conducting structure has been presented. The method differs from the numerous other published methods in the choice of elliptic integrals and their compatibility with the numeric solution. This method was developed to assist in the simulation of a multi-segment variable-pitch helical magnetocumulative generator.

Manuscript received December 5, 2002

## References

[1] Novak B.M., Smith I.R., Enache M.C., and Stewardson H.R. Simple 2D model for helical flux-compression generators // Laser and Particle Beams. – 1997. – V. 15, N 3. – P 379.

[2] Grover F.W. Inductance Calculations. – New York: Dover. – 1962. – 77 p.

[3] Smythe W.R. Static and Dynamic Electricity. – McGraw-Hill. – 1968. – 290 p.

[4] Knoepfel H.E. Magnetic Fields. – Wiley & Sons. – 2000. – 123 p.

[5] Altgilbers L.L., Brown M.D.J., Grishnaev I., Novac B.M., Smith I.R., Tkatch Yu.V, Tkatch Ya.Yu. Magnetocumulative Generators. – Springer. – 2000. – 254 p.

[6] Press W.H., Flannery B.P., Teukolsky, Vetterling W.T. Numerical Recipes in Pascal. – Cambridge University Press. – 1989. – 205 p.

[7] Kaufman M., Seidman A. Handbook for Electronics Engineering Technicians. – McGraw-Hill. – 1984. – P. 3–3.